Journal of Physics: Conference Series

**PAPER** • **OPEN ACCESS**

# Fabrication of aqueous colloids of $Ti_xO_{2x-1}$ and Ag composite nanostructures by means of pulsed laser processing

To cite this article: N E Stankova *et al* 2021 *J. Phys.: Conf. Ser.* **1859** 012013

# Fabrication of aqueous colloids of $Ti_xO_{2x-1}$ and Ag composite nanostructures by means of pulsed laser processing

**N E Stankova[1], A Nikolov[1], D Karashanova[2], N Nedyalkov[1], A Dikovska[1], T Milenov[1], C Ristoscu[3], M Badiceanu[3,4] and I N Mihailescu[3]**

[1] Institute of Electronics, Bulgarian Academy of Sciences, 72 Tsarigradsko Chaussee Blvd., Sofia 1784, Bulgaria,
[2] Institute of Optical Materials and Technologies, Bulgarian Academy of Sciences, Acad. Georgy Bonchev Str., 1113 Sofia, Bulgaria,
[3] National Institute for Lasers, Plasma and Radiation Physics, PO Box MG-36, RO-77125, Magurele, Ilfov, Romania,
[4] Faculty of Physics, University of Bucharest, RO-77125, Magurele, Ilfov, Romania

E-mail: nestankova@yahoo.com; stankova@ie.bas.bg

**Abstract**. Pulsed laser ablation in liquids is utilized for preparation of composite nanostructures on the basis of $Ti_xO_{2x-1}$ and Ag. Plates of bulk Ti and Ag immersed in the corresponding liquid serve as targets in the ablation procedure. A nanosecond Nd:YAG pulsed laser is employed as a source of irradiation. Its fundamental wavelength and the third and fourths harmonic are used both to fabricate and to change the chemical composition and the morphology of the nanostructures considered. The procedure for synthesis of complex nanostructures is performed following a specific sequence, namely, the consecutive laser ablation of the selected targets is followed by a post-ablation irradiation of the colloid obtained of the complex nanostructures. The changes in the characteristics of the complex nanostructures are indirectly evaluated based on the profile of the optical transmission spectra of the as-obtained colloids. The colloids' properties are controlled by varying the laser beam parameters. Transmission electron microscopy (TEM) is applied for direct visualization of their shape. The chemical composition and the morphology were assessed by high-resolution TEM and SAED analyses.

## 1. Introduction

Various photocatalytic processes have gained particular research attention in terms of their various environmental applications related to effective pollution control, sustainable energy production, and improvement of the quality of life. There has been an increasing interest in integrating noble metal or bimetals (Au, Ag or Pd) and titania in nanoscale architectures because of the plasmon-induced enhancement of their photovoltaic efficiency and photocatalytic activity [1-3]. On the one hand, this is because $TiO_2$ is one of the most interesting photocatalysts among the semiconductor oxides [4, 5]. On the other, the noble metal additives are believed to play an essential role in affecting the direct generation of photocurrent based on their localized surface plasmon resonance (LSPR) in the visible spectral range. They provide easy electron transport out of the $TiO_2$ structure by minimizing the electron-hole recombination in the photocatalytic process. The contribution has been studied intensively of the noble-metal particles to the formation of Schottky barriers at the interfacial contact area of noble metal/$TiO_2$ nanostructures under UV and visible light excitation [1-7]. Such hybrid nanostructures can be activated

by absorption not only of UV light, but also of visible light, which extends the optical response of $TiO_2$ to the visible spectral range. Based on this phenomenon, many applications have been proposed of the photocatalytic properties of $Ag/TiO_2$ nanostructures, such as water treatment, air purification from odors, gases and bacteria, $H_2$ production [8-10]. Due to the synergistic antibacterial effect of both Ag and $TiO_2$, such hybrid nanoparticles have been used as biocides and in other medical applications [11-13].

Various technologies for fabrication of $Ag/TiO_2$ hybrid nanostructures have been developed. Most of them have usually required complicated equipment and toxic substances (as nitrogen, hydrazine etc.) [14, 15]. One alternative method for a green and relatively inexpensive fabrication process of $Ag/TiO_2$ nanocomposites is the pulsed laser ablation in different environments (vacuum, gases, liquids) [16].

In this work, we report on a fast and cost-effective approach to the production of water colloids of $Ag/Ti_xO_{2x-1}$ nanocomposites by pulsed laser ablation in liquids (PLAL) followed by pulsed laser UV irradiation in liquid (PLIL) by using a nanosecond Nd:YAG laser system. Our aim is to provide information on an easily-controlled method for fabrication of contaminant-free colloidal $Ag/Ti_xO_{2x-1}$ nanocomposites. Data has been previously reported demonstrating the advantages of using oxygen-deficient $Ti_xO_{2x-1}$ in a wide range of applications based on visible light driven response, charge separation, and photocatalitic selectivity [17, 18]. In contrast with the approaches applied by other authors [19, 20] to prepare $Ag/Ti_xO_{2x-1}$ composite nanostructures by PLAL, we avoided additional complicated procedures for isolating, drying and long-time (more than one hour) annealing at high temperatures (> 400°C).

## 2. Materials and Method

The experiments were conducted by following a two-step pulsed laser processing by using a Q-switched nanosecond Nd:YAG laser system (LOTIS) generating pulses with duration of 15 ns at a repetition rate of 10 Hz:

### *2.1. First step – fabrication of initial water colloid of $Ti_xO_{2x-1}$ and Ag nanostructures*

A Ti target was immersed in doubly distilled water (conductivity 0.6 μS $m^{-1}$) and ablated by 5400 consecutive pulses of a focused laser light beam with a wavelength of 1064 nm. The laser beam was directed perpendicularly to the target surface through a lens with a focal distance of $f$ = 22 cm. The laser fluence thus applied was 10.3 J $cm^{-2}$. The target was fixed appropriately to the water container bottom. The container was mounted on a computer-controlled stepper-motor *x-y* table. The speed of motion of the stage provided an operating mode corresponding to ~10 overlapping pulses. Colloidal nanostructures of $Ti_xO_{2x-1}$ were thus obtained. Further, the Ti target was replaced by a Ag target, which was immersed and then ablated in the aqueous colloid of $Ti_xO_{2x-1}$ already produced. The ablation procedure was repeated under the same production conditions, with only the value of the laser fluence being changed to 26.3 J $cm^{-2}$. The initial aqueous colloid of $Ti_xO_{2x-1}$ and Ag nanostructures was thus finally prepared.

### *2.2. Second step – laser-induced modification of the initial colloid of $Ti_xO_{2x-1}$ and Ag nanostructures*

The aqueous colloid of $Ti_xO_{2x-1}$ and Ag nanostructures was divided and stored in two containers. Each colloid was irradiated by an unfocused laser beam of either the third (355 nm) or the fourth harmonic (266 nm) emitted by the same Nd:YAG laser system. The laser beam was directed normally to the colloid top surface. The container was fixed to a stage rotating at a frequency of 4.3 rpm. The two colloids were exposed to the laser irradiation for different total periods of time with the fluence values of 0.09 J $cm^{-2}$ and 0.14 J $cm^{-2}$, respectively. The total time of laser exposure was determined based on the laser treatment effect on the optical transmission spectra of the $Ag/Ti_xO_{2x-1}$ nanocomposite colloid measured at each five minutes of irradiation (see figure 1). The laser parameters, namely, the wavelength and the pulse energy, were determined during preliminary experiments in view of achieving effective changes in the plasmonic properties of the colloids.

### 2.3. *Characterizations of the Ag/$Ti_xO_{2x-1}$ nanocomposite colloids*

An Ocean Optics HR 4000 spectrometer was used to measure the optical transmittance in the UV-Vis range between 200 nm and 900 nm of the $Ti_xO_{2x-1}$ and Ag water colloids nanostructures resulting from the first and the second preparation steps. Transmission electron microscopy (TEM), high-resolution transmission electron microscopy (HRTEM) and selected area electron diffraction (SAED) were applied for structural characterization. We only present below the TEM and SAED images as acquired by a JEOL JEM 2100 apparatus at an accelerating voltage of 200 kV.

## 3. Results and Discussion

Figures 1 (a) and 1 (b) compare the optical transmission spectra of: (i) the $Ti_xO_{2x-1}$ colloidal nanostructures and the initial water colloid obtained after completing the first step of the fabrication, and of (ii) the aqueous colloids of Ag/$Ti_xO_{2x-1}$ nanostructures obtained after the subsequent laser irradiation (during the second step of the procedure). The shape of the optical transmission spectrum of the colloidal nanostructures of $Ti_xO_{2x-1}$ is typical for the one usually observed for thin films of $TiO_x$ [18, 21]. A dramatic change in the optical transmission is seen after ablation of the Ag target in the water colloid of $Ti_xO_{2x-1}$. A well-defined and pronounced absorbance band appears (with a maximum at ~ 407 nm), which we attribute to the SPR in the Ag NPs produced in the colloid, figures 1 (a) and 1 (b). The right spectrum wing increases rapidly and extends towards the longer wavelengths, with the initial colloid becoming more and more transparent. The TEM images of the initial colloid presented in figure 2 reveal that silver nanoparticles were formed with a size of less than 100 nm (black particles in the images). Moreover, the formation is evident of flower-like sub-microstructures (grey color) surrounding the silver nanoparticles. They were ascribed to polycrystalline oxygen-deficient phases of $Ti_xO_{2x-1}$ by means of the HRTEM and SAED measurements (not presented here) and the corresponding calculations. Also, the presence was ascertained of polycrystalline cubic phases of silver.

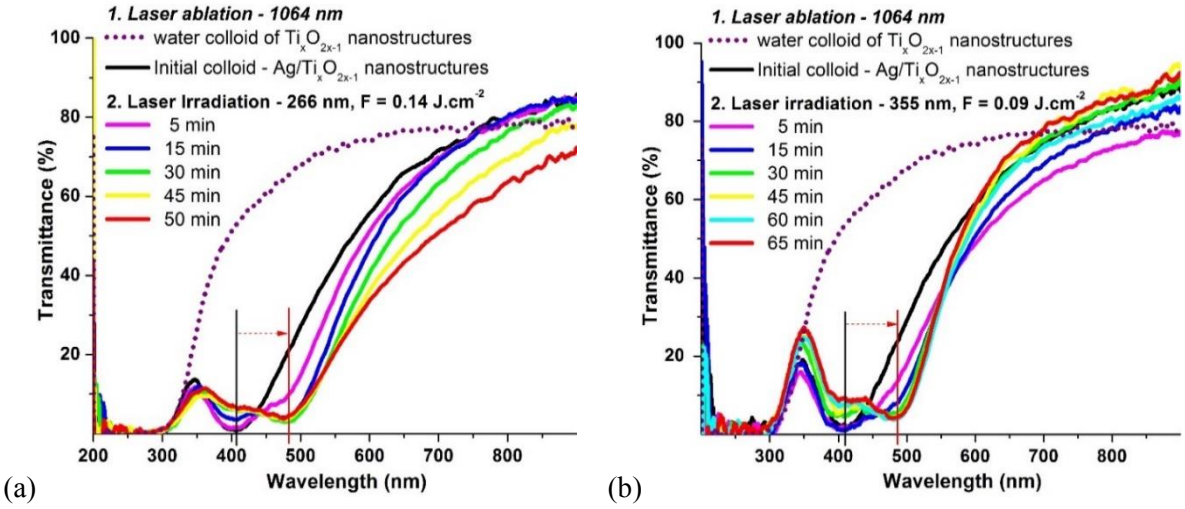


**Figure.1** Optical transmission spectra of the initial colloid and of the Ag/$Ti_xO_{2x-1}$ nanocolloids produced after laser irradiation at (a) 266 nm and (b) 355 nm.

The amount of the as-obtained initial colloid was then divided into two equal parts and each was irradiated by the third harmonic (355 nm) or by the fourth harmonic (266 nm) only, as already described in 2.2. As the second step was performed, the optical transmission was measured after each five-minute laser irradiation.

The total time of laser exposure of each colloid was determined based upon the effect of the irradiation on the optical transmittance spectra observed during the previous step of the laser treatment. The results are presented in figures 1 (a) (2) and 1 (b) (2). A similar behavior of the spectra is seen for

the laser irradiation at the two UV wavelengths. Once the laser irradiation starts, the optical transmittance

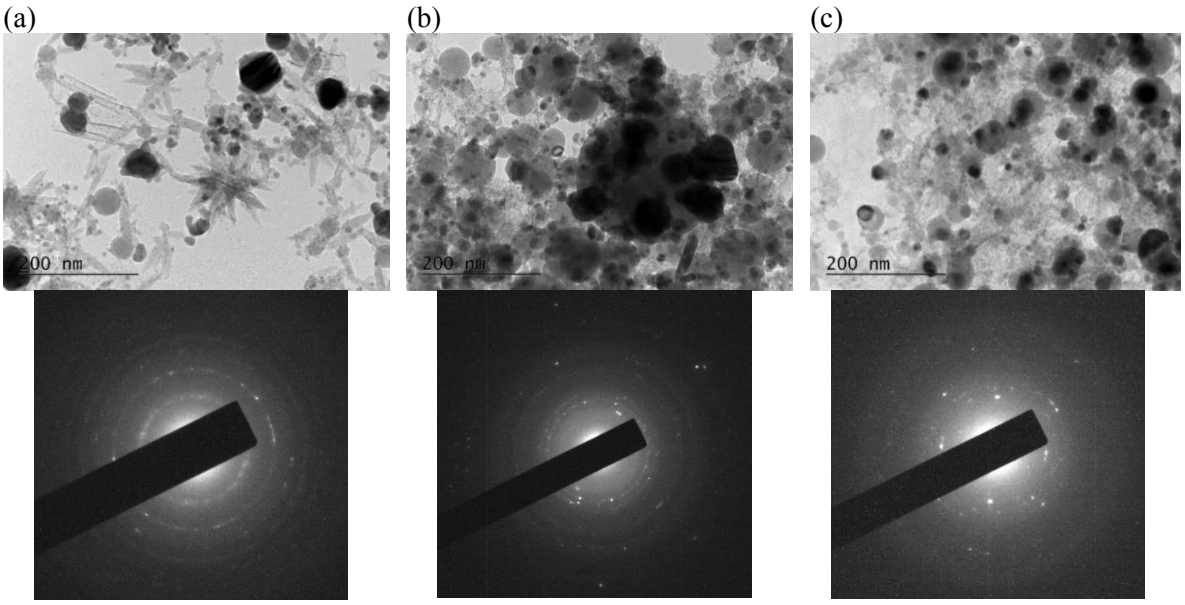


**Figure 2.** TEM micrographs and SAED patterns of Ag/ $Ti_xO_{2x-1}$ nanocolloids: (a) initial colloid after laser ablation at 1064 nm; and subsequent laser irradiation by (b) 266 nm and (c) 355 nm.

of both colloids changes significantly compared with the initial colloid. A second peak with a maximum located at ~ 483 nm appears in the SPR absorbance band. It is red-shifted and more prominent than the first peak, which is located at ~ 407 nm. One possible reason could be the formation of larger Ag NPs. However, in the case of laser treatment at 355 nm, the second band is better defined than the first one in comparison with the case of applying the wavelength of 266 nm. Moreover, as the duration of irradiation increases, the second peak increases significantly and the first one decreases considerably. The comparison of the TEM images (figure 2) of the colloids with nanostructures taken immediately after the laser ablation at 1064 nm (initial colloid) and later after the following irradiation at 355 nm or at 266 nm reveals that larger Ag NPs are much more likely to occur in the initial colloid than in the colloids after the UV laser treatment. It is evident that after 60 minutes of irradiation at 355 nm or after 15 minutes of irradiation at 266 nm, the size of the silver nanoparticles decreases significantly. In both cases, the Ag NPs are mostly smaller than 50 nm and tend to adhere to the surface of the $Ti_xO_{2x-1}$ nanoparticles. The as-formed $Ti_xO_{2x-1}$ nanoparticles appeared to be more than twice as large as the Ag NPs. It is worth noting that the laser irradiation of the initial colloids at the two UV wavelengths induces significant morphological transformation of the $Ti_xO_{2x-1}$ – from flower-like microstructures to very well-defined large spherical nanoparticles. The HRTEM and SAED patterns of these colloids also confirmed the presence of polycrystalline oxygen-deficient phases of $Ti_xO_{2x-1}$ and of cubic polycrystalline metallic silver.

In our previous investigation [22], we found that the post-ablation treatment of water Ag nanocolloids by unfocused laser beams at the wavelengths of 355 nm and/or 266 nm and appropriate laser fluence values leads to a significant fragmentation of the Ag nanoparticles to less than 10 nm. In the present study, the same tendency was observed of reducing the Ag nanoparticles size after treating the initial colloids by unfocused laser beams at the wavelengths of either 355 nm or 266 nm. However, according to the well-established knowledge of the optical properties of metal clusters [23], the smaller the size of the metal nanoparticles, the more the corresponding SPR band peak must be shifted to the shorter wavelengths, and vice versa.

It means that in the present experiments the expected result from the fragmentation of the silver nanoparticles during the irradiation of the initial colloids at 355 nm or at 266 nm should be blue-shifted

relative to their first SPR band peak (i.e., the peak band value should be lower than 407 nm). However, as it is evident, all optical transmission spectra of the UV irradiated colloids taken after each five minutes of laser exposure reveal the tendency of red-shifting of the SPR. We assume that the SPR red-shift of silver nanoparticles observed after UV irradiation is primarily due to the presence of the oxygen-deficient phases $Ti_xO_{2x-1}$ in the colloids. Or, the $Ti_xO_{2x-1}$ medium has a much stronger contribution to the modification of the plasmonic properties of the silver nanoparticles than their size. Also, many publications can be found reporting refractive index values of $TiO_2$ and its oxygen deficient phases over the UV-Vis wavelengths range that are much higher (usually $n > 1.9$) than the values of silver thin films ($n \sim 0.05 - 0.07$) and water ($n \sim 1.36 - 1.33$). Therefore, the $Ti_xO_{2x-1}$ nanoparticles, being a dielectric environment of the as-formed Ag NPs, have a significant effect by moving the second Ag NPs SPR band peak to the lower frequencies (red shift). This effect is strongly supported by the adhesion of the silver nanoparticles to the surface of the larger $Ti_xO_{2x-1}$ nanoparticles, especially in the case of irradiation at the wavelength of 266 nm. We should point out that in the case of irradiation at 355 nm, even after 60 minutes of laser exposure, the first SPR band at ~ 407 nm still exists along with the second one at ~ 483 nm, which could be due to morphological particularities of both Ag and $Ti_xO_{2x-1}$ nanostructures. The morphological and the plasmonic modifications observed result from the synergistic effect of the consecutive application of the fundamental and the UV wavelengths of the Nd:YAG laser. By controlling the laser beam parameters and the time of laser exposure, one could achieve tuning of the SPR band.

The main difference manifested during the UV treatment at the two wavelengths was the total time of laser irradiation needed to obtain this red-shift effect. The second SPR absorbance peak appeared after a 60-minute irradiation at 355 nm and after only 15-minute irradiation at 266 nm. Further laser treatment at 355 nm or 266 nm led to a fast broadening of the SPR band, with the right wing of the optical transmission vanishing.

## 4. Conclusion

This study demonstrates a cost-effective and environmentally-friendly synthesis of aqueous colloidal nanocomposites of Ag/ $Ti_xO_{2x-1}$ by applying a pulsed laser processing at the fundamental (1064 nm) followed by irradiation at either the third or the fourth harmonic wavelengths of a nanosecond Nd:YAG laser system. We found that the consecutive application of the near-infrared and the UV (355 nm or 266 nm) wavelengths induces synergistic effects, which was revealed by dramatic changes in the morphological and in the plasmonic properties of the as-produced Ag/ $Ti_xO_{2x-1}$ nanocomposites.

The characteristics of the Ag/ $Ti_xO_{2x-1}$ nanocolloids prepared can be summarized as follows:

- formation of large silver particles surrounded by flower-like sub-microstructures of oxygen-deficient titanium oxide phases after laser ablation at 1064 nm;
- formation of water colloids of Ag/ $Ti_xO_{2x-1}$ nanocomposites through (i) fragmentation of the silver particles into smaller ones, (ii) formation of well-defined spherical $Ti_xO_{2x-1}$ nanoparticles (iii) on the surface of which Ag nanoparticles adhere after the subsequent post-ablation UV (355 nm or 266 nm) laser irradiation of the initial colloids;
- extension of the optical response (SPR band peak at ~407 nm) of the Ag/$Ti_xO_{2x-1}$ nanocomposites to the longer wavelengths (SPR band peak at ~487 nm).
- stronger influence of the 266-nm wavelength on the morphological and, hence, on the plasmonic properties of the Ag/$Ti_xO_{2x-1}$ nanocomposites compared to that of the 355-nm wavelength;
- the local SPR band of Ag NPs is affected primarily by the higher dielectric constant of the titanium oxides medium, rather by the size of the silver nanoparticles;
- triclinic $Ti_xO_{2x-1}$ and cubic Ag phases are formed after laser processing at 1064 nm, 266 nm and 355 nm.

Further studies are planned on the influence of the laser beam parameters on the structural modification of water colloidal ensembles of noble metals and $Ti_xO_{2x-1}$ nanostructures and the resulting optical characteristics and photocatalytic properties.

The results obtained are promising in terms of applying a simple processing approach to the fabrication of contaminant-free Ag/$Ti_xO_{2x-1}$ nanocomposites with tunable plasmonic and morphological characteristics, thus finding applications optoelectronics as photocatalysts, as photo-electrodes for solar energy harvesting, and in the biomedicine.

**Acknowledgments**
The authors acknowledge the financial support of the Bulgarian National Science Fund under project KP-06-N37/20 "Formation and physical properties of composite nanostructures of metal oxides and noble metals". The bilateral cooperation (2020-2022) between the Romanian and the Bulgarian Academies of Sciences is also acknowledged. Research equipment of distributed research infrastructure INFRAMAT (part of the Bulgarian National Roadmap for Research Infrastructures) supported by the Bulgarian Ministry of Education and Science under contract D01-284/17.12.2019 was used in this investigation.

**References**
[1] Sahu G, Wang K, W Gordon Sc, Zhou W and Tarr M A 2012 *RSC Adv.* **2** 3791
[2] Kochveedu S Th, Kim D-P and Kim D Ha 2012 *J. Phys. Chem.* **116** 2500
[3] Lokman M Q, Shafie S, Shaban S, Ahmad F, Jaafar H, Rosnan R M, Yahaya H and Abdullah S S 2019 *Materials* **12 (13)** 2111
[4] Petronella F, Truppi A, Ingrosso C, Placido T, Striccoli M, Curri M L, Agostiano A and Comparelli R 2017 *Catalysis Today* **281 (1)** 85
[5] Bak T, Li W, Nowotny J, Atanacio A J and Davis J 2015 *J. Phys. Chem.* A **119** (36) 9465
[6] Wu Xu, Centeno A, Zhang X, Darvill D, Ryan M P, Riley D J, Alford N M and Xie F 2015 *Solar Energy Materials and Solar Cells* **138** 80–85
[7] Haider A J, Thamir A D, Najim A A and Ali G A 2017 *Plasmonics* **12** 105
[8] Zielinska-Jurek A and Zaleska A 2014 *Catal. Today* **230** 104
[9] Kowalska E, Wei Z, Karabiyik B, Herissan A, Janczarek M, Endo M, Markowska-Szczupak A, Remita H and Ohtani B 2015 *Catal. Today* **252** 136
[10] Qu Y, Zhou W, Ren Z, Tian C, Li J and Fu H 2014 C*hemPlusChem* **79** 995
[11] Rosa P F, Alves A C M, Aguiar M L and Bernardo A 2017 *Materials Science Forum* **899** 212
[12] Hidayati N, Barudin A, Sreekantan S, Thong O M and Sahgal G 2013 *Materials Science Forum* **756** 238
[13] Prakash J, Kaith B S, Sun S, Bellucci S and Swart H C 2019 *Microbial Nanobionics*, Nanotechnology in the Life Sciences (Springer Nature Switzerland AG) pp 121
[14] Angkaew S and Limsuwan P 2012 *Procedia Engineering* **32** 649
[15] Ran H, Fan J, Zhang X, Mao J and Shao G 2018 *Appl. Surf. Sci.* **430** 415
[16] Hong R, Shi J, Li Z, Liao J, Tao C, Wang Q, Lin H and Zhang D 2020 *Optical Materials* **109** 110338
[17] Pan X, Yang M-Q, Fu X, Zhang N and Xu Y-J 2013 *Nanoscale* (RSC Publishing) **5** 3601
[18] Chen C H, Shieh J, Hsieh S M, Kuo C L and Liao H Y 2012 *Acta Materials* **60** 6429
[19] Liu C H, Hong M H, Zhou Y, Chen G X, Saw M M and Hor A T S 2007 *Phys. Scr.* **T129** 326
[20] Zhou R, Lin S, Zong H, Huang T, Li F, Pan J and Cui J 2017 *Journal of Nanomaterials* (Hindawi) **2017** Article ID 4604159
[21] Essalhi Z, Hartiti B, Lfakir A, Siadat M and Thevenin P 2016 *J. Mater. Environ. Sci.* **7(4)** 1328
[22] Nikolov A S, Stankova N E, Karashanova D B, Nedyalkov N N, Pavlov E L, Koev K Tz, Najdenski Hr, Kussovski V, Avramov L A, Ristoscu C, Badiceanu M and Mihailescu I N 2020 arXiv:2007.13485 [physics.app-ph]
[23] Amendola V, Bakr O M and Stellacci F 2010 *Plasmonics* **5** 85